32ND INTERNATIONAL COSMIC RAY CONFERENCE, BEIJING 2011

Update of the Search for Gamma Ray Bursts with ARGO-YBJ in Scaler Mode

T. DI GIROLAMO[1], P. VALLANIA[2], C. VIGORITO[3] FOR THE ARGO-YBJ COLLABORATION
[1]*Università di Napoli "Federico II" and INFN-Napoli, Italy*
[2]*IFSI-INAF and INFN-Torino, Italy*
[3]*Università di Torino and INFN-Torino, Italy*
tristano@na.infn.it

Abstract: We report an update of the search for emission from Gamma Ray Bursts (GRBs) in the energy range 1−100 GeV in coincidence with the prompt emission detected by satellites, using the large field of view (about 2 sr) air shower detector ARGO-YBJ, appropriate to monitor unpredictable and short duration events like GRBs. The search has been carried out using the single particle technique in time coincidence with satellite detections both for single events and by stacking GRBs in time and phase. Between December 2004 and April 2011, 131 GRBs detected by different satellites occurred in the ARGO-YBJ field of view (zenith angle within 45 degrees). For 110 of these we searched for a high energy counterpart in the ARGO-YBJ data, finding no statistically significant signal. The resulting fluence upper limits between 1 and 100 GeV reach values as low as $10^{-5} erg/cm^2$, and in one case (GRB090902B) can be compared with observations by the LAT instrument on the Fermi satellite.

Keywords: gamma ray bursts - gamma ray observations - extensive air showers

1 Introduction

The study of GRBs has been carried out mainly from space detecting directly the primary photons. Due to the fast decrease of their spectrum, the operating energies are usually in the keV−MeV range, and only the EGRET instrument in the past and now AGILE and the Fermi Gamma Ray Space Telescope reached the GeV region, with maximum detectable energies of 30 and 300 GeV, respectively. At ground level, the search can be performed by means of large area extensive air shower detectors operating at high altitude, measuring the secondary particles produced by the interaction of the primary photons with the atmospheric nuclei. This search, started many years ago (see for example [1, 2, 3, 4, 5]) as a particular way to use experiments designed for gamma-ray astronomy, requires very stable and reliable detectors. Moreover, at lower energies the number of secondary particles reaching the ground, often only one, does not allow the measurement of the arrival direction, making unfeasible an independent detection.

More than forty years after their discovery and more than ten years after the detection of the first afterglow by BeppoSAX, the physical origin of the GRBs is still under debate, allowing a variety of theoretical models. In these conditions, and mainly at energies $>$1 GeV, any further result could be of great importance to improve the knowledge of the GRB puzzle. ARGO−YBJ may reveal the spectral cutoff of GRBs and constrain their emission models.

2 The Detector

The ARGO−YBJ experiment is located at the YangBaJing Cosmic Ray Laboratory (Tibet, P.R. China, 30.11°N, 90.53°E, 4300 m a.s.l., atmospheric depth 606 g/cm^2). The detector is constituted by a central carpet large $\sim$74$\times$78 m^2, made of a single layer of Resistive Plate Counters (RPCs), operated in streamer mode, with 93% of active area and enclosed by a guard ring partially ($\sim$20%) instrumented up to $\sim$100$\times$110 m^2. The apparatus has a modular structure, the basic data acquisition element being a "cluster" (5.7$\times$7.6 m^2), made of 12 RPCs (2.85$\times$1.23 m^2 each). Each chamber is read by 80 external strips of 6.75$\times$61.80 cm^2 (the spatial pixels), logically organized in 10 independent pads of 55.6$\times$61.8 cm^2, which represent the time pixels of the detector.

The detector is connected to two independent data acquisition systems, corresponding to operations in "shower mode" and "scaler mode". In shower mode the arrival time and the location of each particle are recorded using the pads, allowing the detailed reconstruction of the shower lateral distribution and of the arrival direction. In scaler mode the total counts of each cluster are obtained adding up the signal coming from its 120 pads. This signal is put in coincidence in a narrow time window (150 ns) and read by four independent scaler channels, measuring the total counting rate of $\geq$1, $\geq$2, $\geq$3 and $\geq$4 pads fired every 0.5 s. The corresponding measured rates are $\sim$40 kHz, $\sim$2 kHz, $\sim$300 Hz and $\sim$120 Hz, respectively. This technique does

not allow the measurement of the energy and arrival direction of the primary gamma rays (the field of view is about 2 sr, only limited by the atmospheric absorption), but the energy threshold can be pushed down to ∼1 GeV, overlapping the highest energies investigated by satellite experiments. Moreover, with four measurement channels sensitive to different energies, in case of positive detection valuable information on the high energy spectrum slope and possible cutoff may be obtained [6].

Since for the GRB search in scaler mode the authentication is only given by the satellite detection, the stability of the detector has to be deeply investigated. Details of this study, together with the determination of the effective area, upper limit calculation and expected sensitivity, can be found in [7].

3 Search for emission from GRBs

The present update collects data from November 2004 (corresponding to the Swift satellite launch) to April 2011, with a detector active area increasing from ∼700 to ∼6600 m^2. During this period, a total of 131 GRBs, selected from the GCN Circulars Archive[1], was inside the ARGO-YBJ field of view (i.e. with zenith angle $\theta \leq 45°$); for 110 of these data were available and have been investigated by searching for a statistically significant excess in the counting rates coincident with the satellite detection. In order to extract the maximum information from the data, two GRB analyses have been implemented:

- search for a signal from every single GRB;
- search for a signal from stacked GRBs.

For both analyses, the first step is the data cleaning and check. For each event, the Poissonian behaviour of the counting rates for the four multiplicity channels ($\geq$1, $\geq$2, $\geq$3, $\geq$4) for all the clusters is checked using the normalized fluctuation function:

$$f = (s - b)/\sigma, \qquad \sigma = \sqrt{b + b/20} \tag{1}$$

in a period of $\pm$12 h around the GRB trigger time. In this formula, s is the number of counts in a time interval of 10 s, b the number of counts in 10 s averaged over a time interval of 100 s before and after the signal, and σ the standard deviation, with about 400 independent samples per distribution. The interval of 10 s has been chosen to avoid any systematic effect due to environment and instrument (such as atmospheric pressure and detector temperature variations). The expected distribution of f is the standard normal function; the clusters giving a distribution with measured $\sigma_f > 1.2$ or with anomalous excesses (i.e. number of entries $> 2\%$) in the tail $f > 3$ in at least one multiplicity channel, are discarded. This guarantees that the data fulfil the requirements on stability and reliability of the detector.

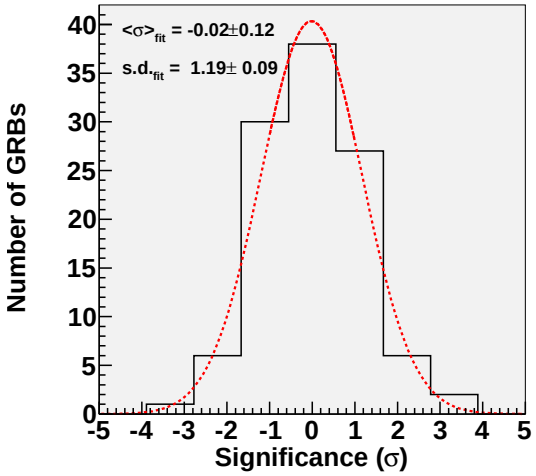

Figure 1: Distribution of the statistical significances of the 110 GRBs with respect to background fluctuations, compared with a Gaussian fit.

3.1 Search for single GRBs

The counting rates of the clusters surviving the quality cuts (∼92%) are added up and the normalized fluctuation function

$$f' = (s' - b')/\sigma', \qquad \sigma' = \sqrt{b' + b' \frac{\Delta t_{90}[s]}{600}} \tag{2}$$

is used to give the significance of the coincident on-source counts. In this formula, s' is the total number of counts in the Δt_{90} time window given by the satellite detector (corresponding to the detection of 90% of the photons) and b' is the number of counts in a fixed time interval of 300 s before and after the signal, normalized to the Δt_{90} time. Due to the correlation between different clusters (given by the air shower lateral distribution), the distributions of the sum of the counts are larger than Poissonian. Taking this into account, the statistical significance of the on-source counts over the background is obtained again in an interval of $\pm$12 h around the GRB trigger time, using equation (17) of [8] (for more details see [7]). All the results are obtained using the single particle counting rate $C_1 = C_{\geq 1} - C_{\geq 2}$, which corresponds to the minimum primary energy in the ARGO-YBJ scaler mode. Figure 1 shows the distribution of the significances for the whole set of 110 GRBs compared with a Gaussian fit, which has mean value -0.02 ± 0.12 and standard deviation 1.19 ± 0.09. No significant excess is shown, and the maximum significance 3.52σ is obtained for GRB080727C, with a chance probability of 2.4% taking into account the total number of GRBs analyzed.

Lacking a positive signal, upper limits to fluence are obtained in the 1-100 GeV energy range adopting a power

1. http://gcn.gsfc.nasa.gov/gcn3_archive.html

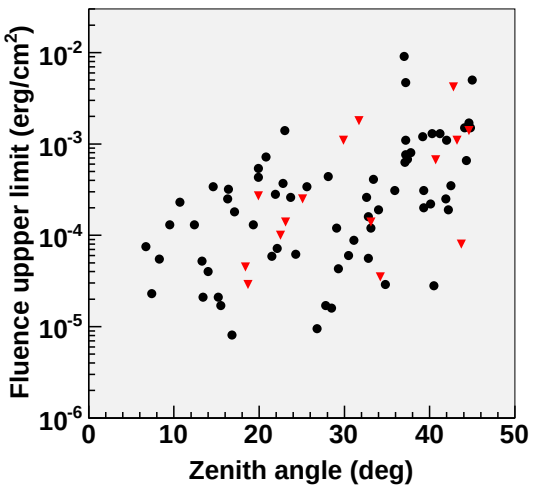

Figure 2: Fluence upper limits as a function of the zenith angle in the 1-100 GeV range, obtained extrapolating the measured keV-MeV spectra. Triangles represent GRBs with measured redshift, circles GRBs assumed at z=1.

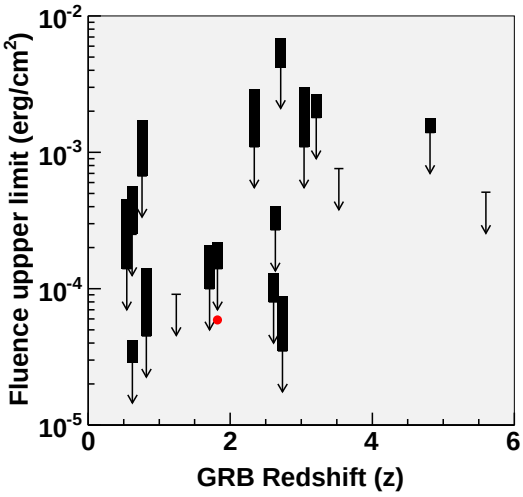

Figure 3: Fluence upper limits of GRBs as a function of redshift. The rectangles represent the values obtained with differential spectral indexes ranging from α=-2.5 to the satellite measurement. The 3 arrows give the upper limits for the former case only (for GRBs with cutoff power law spectrum). The circle shows the integral fluence in the 1-100 GeV range for GRB090902B as observed by LAT.

law spectrum and by considering the maximum number of counts at 99% confidence level (c.l.), following equation (6) in [9]. For this calculation, two different assumptions are used for the power law spectrum: a) extrapolation of the keV-MeV spectrum measured by the satellite experiments, when available; b) a differential spectral index α = -2.5. Since the mean value of spectral indexes measured by EGRET in the GeV energy region is α = -2.0 [10], we expect that the true upper limits lie between these two values. For GRBs with measured redshift, an exponential cutoff in the spectrum is considered to take into account the effect of extragalactic absorption, which is calculated using the values given in [11]. When the redshift is not measured, a value z = 1 is adopted. For the subset of 82 GRBs with spectral index α measured by satellites, the fluence upper limits have been calculated according to assumption a) and they are shown in figure 2 as a function of the zenith angle.

For the subset of 18 GRBs with measured redshift, the fluence upper limits for the two assumed spectra are shown in figure 3. Since the measured low energy differential spectral indexes for these GRBs are always greater than -2.5, the higher upper limits refer to this extrapolation. For 3 GRBs the measured low energy spectrum is a cutoff power law, thus only the value obtained assuming α=-2.5 is shown. For the other GRBs the rectangles indicate the upper limit range corresponding to differential spectral indexes between the fixed value α=-2.5 and the low energy measurement. For GRB090902B the resulting upper limit range can be compared with observations by the LAT instrument on the Fermi satellite (circle in figure 3).

When using as the GRB spectrum the extrapolation of the index measured by satellite experiments, an upper limit to the cutoff energy can be determined at least for some GRBs exploiting the ARGO−YBJ scaler mode data, with the following procedure. The extrapolated fluence is plotted together with the fluence upper limit as a function of the cutoff energy E_{cut}. If the two curves cross in the 2-100 GeV energy range, the intersection gives the upper limit to the cutoff energy. For these GRBs we can state, with a 99% c.l., that their spectra do not extend beyond this value of E_{cut}, if the slope remains constant. Figure 4 shows the resulting cutoff energy upper limits as a function of the spectral index for the 19 GRBs with critical intersection in the quoted energy range. For 4 of these (triangles in figure 4) the measurement of the redshift allows the estimation of the extragalactic absorption. When the GRB redshift is not available, the value z=1 is adopted.

3.2 Stacked analysis

The search for cumulative effects by stacking all the GRBs either in fixed time durations or in phases of Δt_{90} could enhance a possible signal, making it statistically significant, even if the emission of each GRB is below the sensitivity of the ARGO−YBJ detector. In this case, less information could be given compared to the single GRB coincident detection, however we must consider that with the stacked analysis we increase the sensitivity by increasing the number of GRBs, while with the single GRB search we decrease the sensitivity because of the increasing number

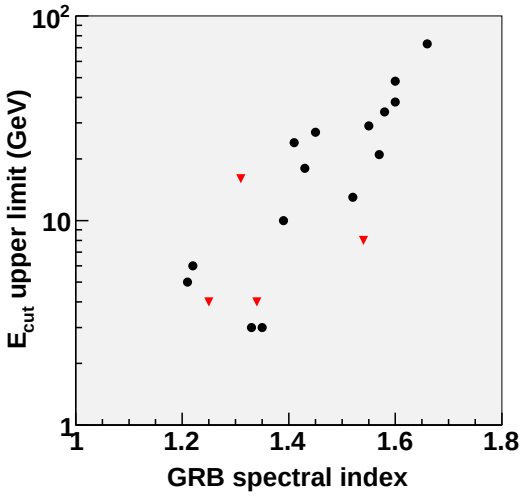

Figure 4: Upper limits to the cutoff energy of GRBs as a function of the spectral index obtained extrapolating the keV-MeV spectra measured by satellites. The triangles represent the values obtained taking into account the extragalactic absorption for the GRBs with measured redshift, for the others z=1 is adopted.

of trials. The stacked analysis is carried out supposing a common timing feature in all GRBs.

First, the total number of counts in a time window Δt (with Δt=0.5, 1, 2, 5, 10, 20, 50, 100, 200 s) after T_0 (the trigger time given by the satellites) for all the GRBs are added up. This is done in order to search for a possible cumulative high energy emission with a fixed duration after T_0. A positive observation at a fixed Δt could be used as an alternative value to the standard Δt_{90} duration. Indications of a delayed high energy component have been observed by satellite experiments in some GRBs. The resulting significances for the 9 time bins give no evidence of emission for a certain Δt. Since the bins are not independent, the distribution of the significances of the 9 time bins is compared with random distributions obtained for starting times different from T_0 in a time window of $\pm$12 h around the true GRB trigger time. The resulting overall significance of the GRBs stacked in time with respect to random fluctuations is -0.57σ.

A second search is carried out to test the hypothesis that the high energy emission occurs at a particular phase of the low energy burst, independently of the GRB duration. For this study, the 92 GRBs with $\Delta t_{90} \geq 5\ s$ (i.e. belonging to the "long GRB" population, defined by $\Delta t_{90} \geq 2\ s$) have been added up in phase after scaling their duration. This choice has been made for both physical and technical reasons, adding up the counts for GRBs of the same class and long enough to allow a phase plot with 10 bins given the time resolution of 0.5 s. No evidence of emission at a certain phase is obtained, and the overall significance of the GRBs stacked in phase (obtained adding up all the bins) with respect to background fluctuations is -0.73σ.

3.3 Conclusions

In this paper we have reported a study concerning the search for GeV photons from 110 GRBs carried out by the ARGO−YBJ air shower detector operated in scaler mode. In the search for GeV gamma rays in coincidence with the lower energy GRBs detected by satellites, no evidence of emission was found for any event. The search for a signal from GRBs stacked both in time and in phase has shown no deviation from the statistical expectations, therefore excluding any integral effect. The obtained upper limits to the fluence in the 1-100 GeV energy range depend on zenith angle, time duration and spectral index, reaching values as low as $\approx 10^{-5} erg/cm^2$, in the case of GRB090902B a value just a factor about 3 higher than the fluence extrapolated from LAT observations. Since upper limits to the cutoff energy can be set for several GRBs between 2 and 100 GeV, we confirm that the simple extrapolation of the power law spectrum measured at low energies is not always possible [12].

References

[1] O'Brien S., Porter N.A., Astrophysics and Space Science, 1976, **42**: 73-76
[2] Morello C., Periale L., Navarra G., Il Nuovo Cimento C, 1984, **7**: 682-688
[3] Alexandreas D.E. et al., The Astrophysical Journal, 1994, **426**: L1-L3
[4] Castellina A. et al., Proceedings of the 27th ICRC, 2001, 2735-2738
[5] Aglietta M. et al., The Astrophysical Journal, 1996, **469**: 305-310
[6] Aielli G. et al., The Astrophysical Journal, 2009, **699**: 1281-1287
[7] Aielli G. et al., Astroparticle Physics, 2008, **30**: 85-95
[8] Li T., Ma Y., The Astrophysical Journal, 1983, **272**: 317-324
[9] Helene O., Nuclear Instruments and Methods, 1983, **212**: 319-322
[10] Dingus B.L., Catelli J.R., Schneid E.J., Proceedings of the 25th ICRC, 1997, **3**: 29-32
[11] Kneiske T.M. et al., Astronomy and Astrophysics, 2004, **413**: 807-815
[12] D. Band et al., The Astrophysical Journal, 1993, **413**: 281-292